Acta Crystallographica Section C
Structural Chemistry
ISSN 2053-2296

Hirshfeld surface analysis of the 1,1′-(ethane-1,2-diyl)dipyridinium dication in two new salts: perchlorate and peroxodisulfate

Mostafa Gholizadeh, Mehrdad Pourayoubi, Masoumeh Farimaneh, Atekeh Tarahhomi, Michal Dušek and Václav Eigner

Acta Cryst. (2014). C**70**, 230–235

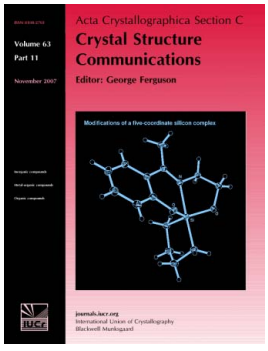

Acta Crystallographica Section C: Structural Chemistry specializes in the rapid dissemination of high-quality detailed studies of novel and challenging crystal and molecular structures of interest in the fields of chemistry, biochemistry, mineralogy, pharmacology, physics and materials science. The unique checking, editing and publishing facilities of the journal ensure the highest standards of structural reliability and presentation, while providing for reports on studies involving special techniques or difficult crystalline materials. Papers go beyond reporting the principal numerical and geometrical data, and may include the discussion of multiple related structures, a detailed description of non-routine structure determinations, placing the structure in an interesting scientific, physical or chemical context, or the discussion of interesting physical properties or modes of association. Reports of difficult or challenging structures, such as cases of twinning, severe disorder, or diffuse solvent regions are welcomed, provided the presented structures are correct and the difficulties and strategies used to treat them are scientifically discussed and properly documented. *Section C* readers have access to an extensive back archive of high-quality structural data.

Acta Crystallographica Section C
Structural Chemistry
ISSN 2053-2296

Hirshfeld surface analysis of the 1,1′-(ethane-1,2-diyl)dipyridinium dication in two new salts: perchlorate and peroxodisulfate

Mostafa Gholizadeh,[a]* Mehrdad Pourayoubi,[a] Masoumeh Farimaneh,[a] Atekeh Tarahhomi,[a] Michal Dušek[b] and Václav Eigner[b]

[a]Department of Chemistry, Ferdowsi University of Mashhad, Mashhad, Iran, and [b]Institute of Physics, Academy of Sciences of the Czech Republic v.v.i., Na Slovance 2, 182 21 Praha 8, Czech Republic
Correspondence e-mail: m_gholizadeh@um.ac.ir

Received 26 October 2013
Accepted 9 January 2014

In the title salts, $C_{12}H_{14}N_2^{2+}\cdot 2ClO_4^-$, (I), and $C_{12}H_{14}N_2^{2+}\cdot S_2O_8^{2-}$, (II), the dication is organized around an inversion centre located at the centre of the $-CH_2CH_2-$ bridge and the two pyridine segments are *anti* with respect to one another. The peroxodisulfate anion in (II) also exhibits inversion symmetry. Hirshfeld surface analysis shows closely similar Hirshfeld surface shapes for the dications in the two salts, reflecting similar intermolecular contacts and similar conformations. The two-dimensional fingerprint plots (FPs) are quite asymmetric, due to the presence of more than one component (cation and anion). The most striking of the complementary features for each of the FPs of the dications is the broad green spike in the region $d_e > d_i$, without the presence of a corresponding spike in the region $d_e < d_i$, reflecting the absence of O···H contacts. Moreover, H···O interactions (51% in the dications of both salts) outnumber other contacts in both crystal structures.

Keywords: crystal structure; Hirshfeld surface analysis; fingerprint plots; 1,1′-(ethane-1,2-diyl)dipyridinium dication; perchlorate salt; peroxodisulfate salt.

1. Introduction

Hirshfeld surface analysis is a very useful tool for the investigation of intermolecular interactions in crystal structures, allowing easy comparison of intermolecular contacts relative to van der Waals radii by a strategy based on a simple colouring scheme (Rohl *et al.*, 2008; Tarahhomi *et al.*, 2013). Such an analysis may be used in the case of symmetry-independent molecules within one structure, analogous structures, cation–anion compounds and polymorphs (Tarahhomi *et al.*, 2013; Ling *et al.*, 2010).

When comparing the crystal structures of cation–anion compounds with one identical component (cation or anion), Hirshfeld surfaces (HSs; Spackman & Byrom, 1997; Spackman & Jayatilaka, 2009; McKinnon *et al.*, 2004) and fingerprint plots (FPs; Spackman & McKinnon, 2002; McKinnon *et al.*, 2004) may be used for elucidating and comparing the intermolecular interactions involved in the crystal packing.

In organic synthesis, some cation–anion compounds based on organic cations and oxidant anions can be employed to improve the selectivity and mildness, and therefore the effectiveness, of the oxidant species, especially in the oxidation of complex and highly sensitive compounds (Bobbitt, 1998). There are some reported structures of such cation–anion compounds, for example, the 1,1′-(ethane-1,2-diyl)dipyridinium dication with dichromate(VI) (Gholizadeh *et al.*, 2012) and iodate anions (Gholizadeh *et al.*, 2011).

Here, we present the syntheses and crystal structures of two new salts of the 1,1′-(ethane-1,2-diyl)dipyridinium dication, namely the bis(perchlorate) salt, (I), and the hexaoxo-μ-peroxo-disulfate(2−) (also known as peroxodisulfate) salt, (II). Hirshfeld surface analysis, using the *CrystalExplorer* software (Wolff *et al.*, 2012), was used to investigate and compare the intermolecular interactions, *viz.* the H···H, H···O, H···C and C···H contacts, in (I) and (II).

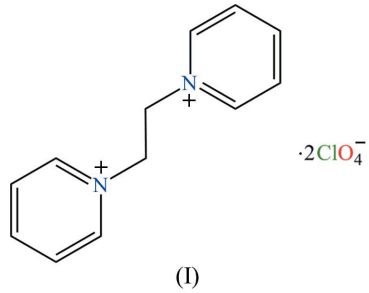

(I)

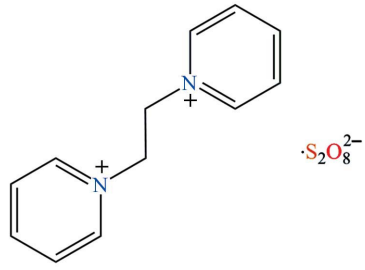

(II)

2. Experimental

2.1. Synthesis and crystallization

1,1′-(Ethane-1,2-diyl)dipyridinium dibromide, $(C_{12}H_{14}N_2)Br_2$, was prepared as described previously (Gholizadeh *et al.*, 2011). The preparation of both (I) and (II) is identical, with the exception of the salts used for providing the counter-anions. To a solution of $(C_{12}H_{14}N_2)Br_2$ (10 mmol) in water (25 ml), an aqueous solution (25 ml) of $KClO_4$ (20 mmol) for (I) or an aqueous solution of $K_2S_2O_8$ (10 mmol) for (II) was added and the resulting solution stirred at room temperature. For both compounds, after 1 h, the precipitate was filtered off,

  doi:10.1107/S2053229614000576

Table 1
Experimental details.

	(I)	(II)
Crystal data		
Chemical formula	$C_{12}H_{14}N_2^{2+}\cdot 2ClO_4^-$	$C_{12}H_{14}N_2^{2+}\cdot S_2O_8^{2-}$
M_r	385.15	378.4
Crystal system, space group	Triclinic, $P\overline{1}$	Monoclinic, $P2_1/c$
Temperature (K)	120	120
a, b, c (Å)	6.0687 (3), 6.7263 (4), 9.8005 (3)	8.2189 (5), 9.6676 (6), 9.8361 (4)
α, β, γ (°)	97.858 (4), 95.503 (4), 100.655 (4)	90, 98.359 (4), 90
V (Å^3)	386.44 (3)	773.24 (7)
Z	1	2
Radiation type	Mo $K\alpha$	Mo $K\alpha$
μ (mm^{-1})	0.47	0.39
Crystal size (mm)	0.57 × 0.31 × 0.17	0.76 × 0.63 × 0.54
Data collection		
Diffractometer	Agilent Xcalibur Gemini Ultra diffractometer with an Atlas detector	Agilent Xcalibur Gemini Ultra diffractometer with an Atlas detector
Absorption correction	Analytical (*CrysAlis PRO*; Agilent, 2010)	Analytical (*CrysAlis PRO*; Agilent, 2010)
T_{min}, T_{max}	0.88, 0.946	0.801, 0.845
No. of measured, independent and observed $[I > 3\sigma(I)]$ reflections	6178, 1904, 1717	5426, 1848, 1687
R_{int}	0.019	0.017
$(\sin\theta/\lambda)_{max}$ (Å^{-1})	0.689	0.689
Refinement		
$R[F^2 > 3\sigma(F^2)]$, $wR(F^2)$, S	0.030, 0.104, 1.79	0.028, 0.092, 1.71
No. of reflections	1904	1848
No. of parameters	110	110
H-atom treatment	H-atom parameters constrained	H-atom parameters constrained
$\Delta\rho_{max}$, $\Delta\rho_{min}$ (e Å^{-3})	0.29, −0.33	0.31, −0.27

Computer programs: *CrysAlis PRO* (Agilent, 2010), *SIR2002* (Burla *et al.*, 2003), *DIAMOND* (Brandenburg & Putz, 2005), *JANA2006* (Petříček *et al.*, 2006), *enCIFer* (Allen, *et al.*, 2004) and *PLATON* (Spek, 2009).

washed with water and recrystallized from H_2O–dimethylformamide (1:1 *v*/*v*) at room temperature.

2.2. Refinement

Crystal data, data collection and structure refinement details are summarized in Table 1. For (I) and (II), all H atoms were placed in calculated positions, with C—H = 0.96 Å (aromatic and CH_2) and $U_{iso}(H) = 1.2U_{eq}(C)$. The data-reduction program *CrysAlis PRO* (Agilent, 2010) discarded two low-angle reflections [001 for (I) and 100 for (II)]. They were recorded in positions close to the beam stop or the Lorentz area of the CCD detector.

3. Results and discussion

In the title bis(perchlorate), (I) (Fig. 1), and peroxodisulfate, (II) (Fig. 2), salts, the dications are organized around an inversion centre located at the centre of the $-CH_2CH_2-$ bridge and the two pyridine segments are *anti* with respect to one another. The pyridinium rings are parallel in both cases, but

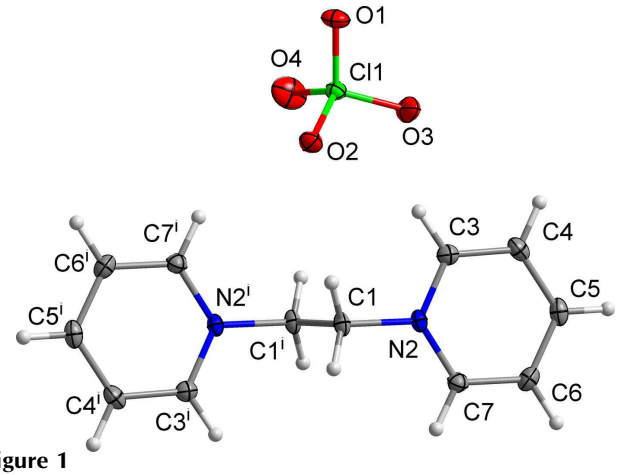

Figure 1
The molecular structure of (I), showing the atom-labelling scheme. Displacement ellipsoids are drawn at the 50% probability level. Symmetry-related atoms are generated by a crystallographic inversion centre. [Symmetry code: (i) $-x, -y+1, -z$.]

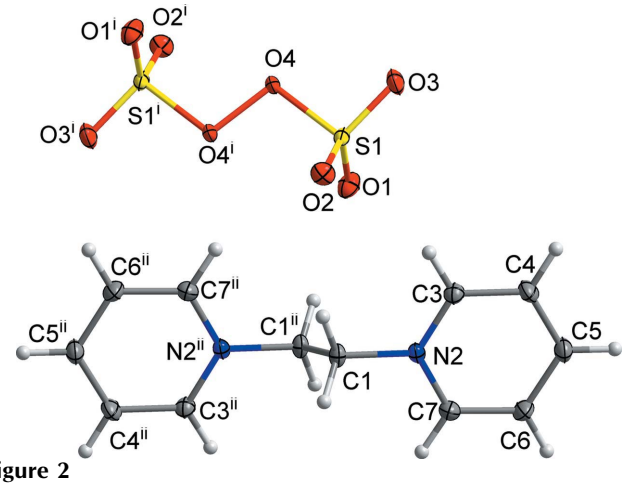

Figure 2
The molecular structure of (II), showing the atom-labelling scheme. Displacement ellipsoids are drawn at the 50% probability level. Symmetry-related atoms are generated by crystallographic inversion centres. [Symmetry codes: (i) $-x+1, -y, -z$; (ii) $-x+1, -y+1, -z$.]

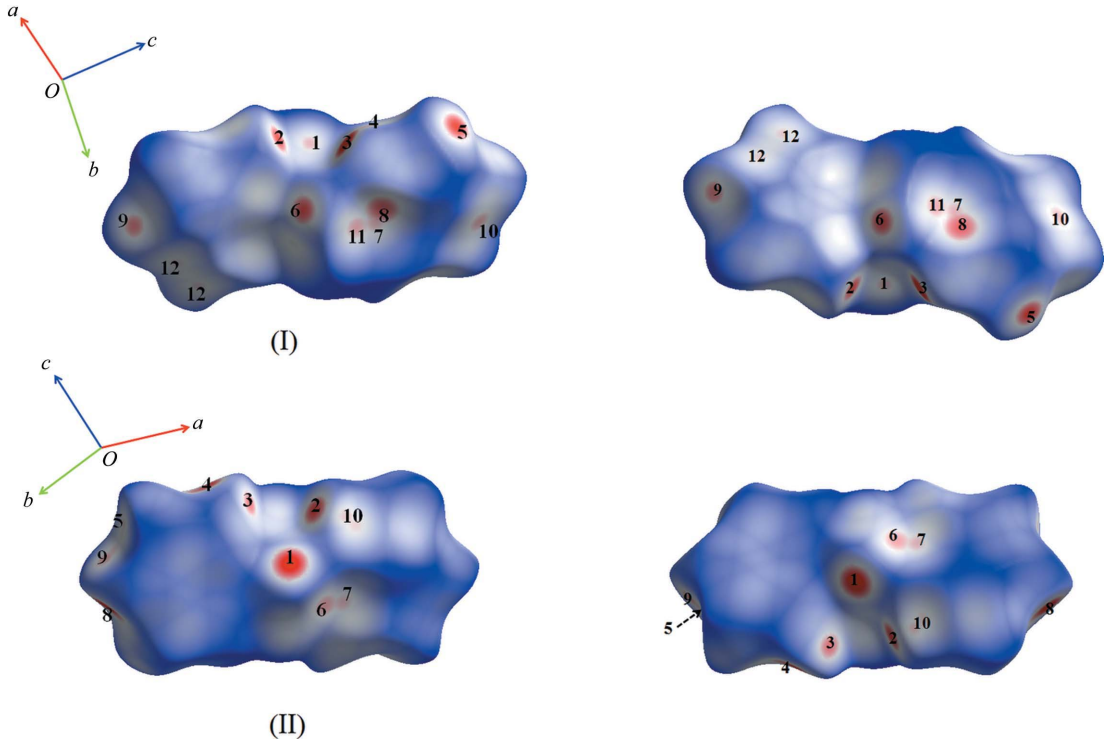

Figure 3
Views of the Hirshfeld surfaces (HSs) in two orientations for the dications of (I) and (II) (HSs mapped with d_{norm}). The labels on the HSs are as follows. For (I), (**1**) C3—H1*C*3···O2; (**2**) C7—H1*C*7···O2^{i}; (**3**) C1—H2*C*1···O2^{i}; (**4**) C3—H1*C*3···O3; (**5**) C4—H1*C*4···O3^{ii}; (**6**) C1—H1*C*1···O2^{iii}; (**7**) C3···O4^{iv}; (**8**) N2···O4^{iv}; (**9**) C1—H1*C*1···O4^{iv}; (**10**) C5···C5^{v}; (**11**) C5—H1*C*5···O3^{vi}; (**12**) C5···C4^{vi}. For (II), (**1**) C1—H2*C*1···O1^{ii}; (**2**) C7—H1*C*7···O2^{ii}; (**3**) C3—H1*C*3···O2; (**4**) C3—H1*C*3···O1^{iii}; (**5**) C7—H1*C*7···O4^{iv}; (**6**) C1—H1*C*1···O2; (**7**) N2···O2^{v}; (**8**) C5—H1*C*5···O1^{vi}; (**9**) C5—H1*C*5···O3^{vii}; (**10**) C4—H1*C*4···O3^{vii}. The symmetry codes are as in Tables 3 and 5.

Table 2
Selected geometric parameters (Å, °) for (I).

Cl1—O1	1.4381 (12)	N2—C1	1.4835 (18)
Cl1—O2	1.4510 (13)	N2—C3	1.347 (2)
Cl1—O3	1.4374 (13)	N2—C7	1.341 (2)
Cl1—O4	1.4332 (13)		
O1—Cl1—O2	109.06 (7)	O3—Cl1—O4	110.09 (8)
O1—Cl1—O3	109.45 (7)	C1—N2—C3	117.85 (13)
O1—Cl1—O4	109.70 (8)	C1—N2—C7	120.22 (12)
O2—Cl1—O3	108.85 (8)	C3—N2—C7	121.93 (13)
O2—Cl1—O4	109.68 (7)		
C3—N2—C1—C1^{i}	83.48 (15)	C4—C3—N2—C1	−179.44 (13)
C7—N2—C1—C1^{i}	−96.28 (15)	C6—C7—N2—C1	178.73 (13)

Symmetry code: (i) $-x, -y+1, -z$.

Table 3
Hydrogen-bond geometry (Å, °) for (I).

D—H···*A*	*D*—H	H···*A*	*D*···*A*	*D*—H···*A*
C3—H1*C*3···O2	0.96	2.38	3.263 (2)	152
C7—H1*C*7···O2^{i}	0.96	2.48	3.3322 (18)	148
C1—H2*C*1···O2^{i}	0.96	2.60	3.326 (2)	132
C3—H1*C*3···O3	0.96	2.58	3.220 (2)	125
C4—H1*C*4···O3^{ii}	0.96	2.47	3.3792 (19)	159
C1—H1*C*1···O2^{iii}	0.96	2.50	3.3888 (19)	155
C3···O4^{iv}			3.000 (2)	
N2···O4^{iv}			2.997 (2)	
C1—H1*C*1···O4^{iv}	0.96	2.63	3.129 (2)	113
C5···C5^{v}			3.297 (2)	
C5—H1*C*5···O3^{vi}	0.96	2.53	3.245 (2)	132
C5···C4^{vi}			3.354 (2)	

Symmetry codes: (i) $-x, -y+1, -z$; (ii) $-x+1, -y+1, -z+1$; (iii) $-x+1, -y+1, -z$; (iv) $x, y+1, z$; (v) $-x, -y+2, -z+1$; (vi) $-x, -y+1, -z+1$.

Table 4
Selected geometric parameters (Å, °) for (II).

S1—O1	1.4374 (10)	N2—C7	1.3447 (17)
S1—O2	1.4408 (9)	N2—C3	1.3485 (17)
S1—O3	1.4388 (11)	N2—C1	1.4757 (16)
O4—O4^{i}	1.4839 (13)		
O1—S1—O2	113.52 (6)	C7—N2—C3	121.85 (11)
O1—S1—O3	115.79 (6)	C7—N2—C1	118.80 (11)
O2—S1—O3	115.85 (6)	C3—N2—C1	119.32 (11)
C3—N2—C1—C1^{ii}	107.08 (12)	O1—S1—O4—O4^{i}	61.05 (8)
C7—N2—C1—C1^{ii}	−74.94 (14)	O2—S1—O4—O4^{i}	−59.71 (8)
C4—C3—N2—C1	178.41 (12)	O3—S1—O4—O4^{i}	−179.30 (7)
C6—C7—N2—C1	−178.69 (12)		

Symmetry codes: (i) $-x+1, -y, -z$; (ii) $-x+1, -y+1, -z$.

Table 5
Hydrogen-bond geometry (Å, °) for (II).

D—H···*A*	*D*—H	H···*A*	*D*···*A*	*D*—H···*A*
C1—H2*C*1···O1^{ii}	0.96	2.36	3.3198 (17)	173
C7—H1*C*7···O2^{ii}	0.96	2.45	3.3552 (17)	158
C3—H1*C*3···O2	0.96	2.52	3.279 (2)	136
C3—H1*C*3···O1^{iii}	0.96	2.41	3.0715 (16)	126
C7—H1*C*7···O4^{iv}	0.96	2.59	3.185 (2)	120
C1—H1*C*1···O2	0.96	2.71	3.358 (2)	125
N2···O2^{v}			2.996 (1)	
C5—H1*C*5···O1^{vi}	0.96	2.34	3.063 (2)	131
C5—H1*C*5···O3^{vii}	0.96	2.54	3.177 (2)	124
C4—H1*C*4···O3^{vii}	0.96	2.60	3.204 (2)	121

Symmetry codes: (ii) $-x+1, -y+1, -z$; (iii) $x, -y+\frac{1}{2}, z+\frac{1}{2}$; (iv) $x, y+1, z$; (v) $-x+1, y+\frac{1}{2}, -z+\frac{1}{2}$; (vi) $-x, -y+1, -z$; (vii) $-x, y+\frac{1}{2}, -z+\frac{1}{2}$.

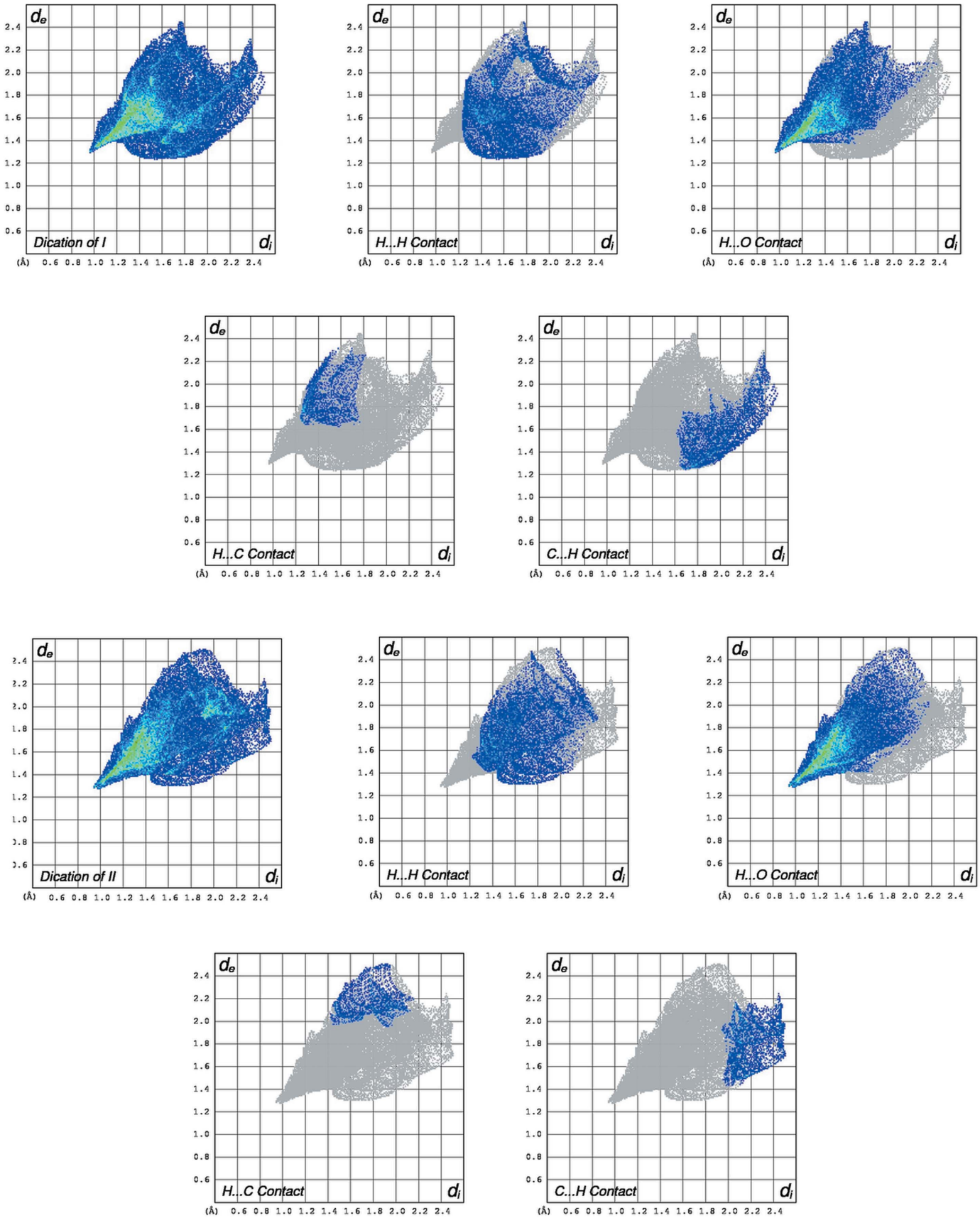

Figure 4
Full fingerprint plots (FPs) for the dications of (I) and (II), and FPs resolved into H···H, H···O, H···C and C···H close contacts. The first two rows are related to the dication of (I), and the third and fourth rows are related to the dication of (II).

the perpendicular distances between their extended planes are 1.486 (2) Å for (I) and 1.309 (4) Å for (II). This difference in the perpendicular distances of (I) and (II) is related to the difference in the angle between the plane of the pyridinium ring and the plane defined by atoms N2/C1/C1^{i}/N2^{i} for (I) [symmetry code: (i) $-x$, $-y+1$, $-z$] and N2/C1/C1^{ii}/N2^{ii} for (II) [symmetry code: (ii) $-x+1$, $-y+1$, $-z$]. The angle between these planes of 83.76 (15)° in (I) is closer to 90° than that of 73.88 (14)° in (II), thus allowing for a larger separation of the pyridinium rings. The peroxodisulfate anion in (II) also exhibits inversion symmetry. The Cl atom in (I) and the S atom in (II) are in tetrahedral environments. Selected bond lengths and angles for (I) and (II) are given in Tables 2 and 4, respectively. The crystal packing in both structures is stabilized by C—H···O hydrogen bonds (Tables 3 and 5).

For the dications of (I) and (II), the three-dimensional Hirshfeld surface (HS) maps are given in Fig. 3; contacts with distances equal to the sum of the van der Waals radii are shown in white, and contacts with distances shorter than or longer than the related sum values are shown in red (highlighted contacts) or blue, respectively. Tables 3 and 5 list the short intermolecular contacts with distances shorter than the sum of the van der Waals radii, and these are identified with red spots on the HSs and labels as defined in Fig. 3. The shapes of the HSs of the dications in both structures are similar, reflecting similar intermolecular contacts (Tables 3 and 5) and similar conformations.

In the crystal packing, the dication of (I) takes part in different intermolecular contacts, *viz.* C—H···O (labels **1**–**6**, **9** and **11** in Fig. 3), C···O (label **7**), C···C (labels **10** and **12**) and N···O (label **8**), and the dication of (II) is involved in intermolecular C—H···O interactions (all labels except **7**) and N···O (label **7**) contacts. In both structures, each dication participates in some similar C—H···O hydrogen bonds, labelled in Fig. 3 as **2**, **3**, **5**, **6** and **9** (Tables 3 and 5). The dark-red spots are related to the shorter C—H···O hydrogen bonds for both structures, and also to the C3···O4 interaction for (I). The light-red spots on the HSs include other intermolecular interactions (Fig. 3, and Tables 3 and 5).

Fig. 4 illustrates the analysis of the two-dimensional fingerprint plots (FPs) for the dications of (I) and (II). FPs are the two-dimensional representations of the information provided by visual inspection of the HSs, which are plotted on an evenly spaced grid formed by (d_e,d_i) pairs, in which d_e and d_i represent the distances from a point on the HS to the nearest atoms outside and inside the surface, respectively. Each grid point is coloured according to the frequency of occurrence of the (d_e,d_i) pair on the HS, from blue for small contributions, through green to red for maximum contributions, if present. For a better identification of different H···*X* or *X*···H (*X* = H, O or C) contacts, the FP of each dication in (I) and (II) is decomposed into H···*X* (and *X*···H)-interactions-only fingerprints.

The two-dimensional fingerprint plots in Fig. 4 are quite asymmetric; this is expected, since interactions occur between two different species (cation and anion). In other words, the asymmetry about the plot diagonal is typical of structures that contain more than one component (molecule/ion) (Fabbiani *et al.*, 2011).

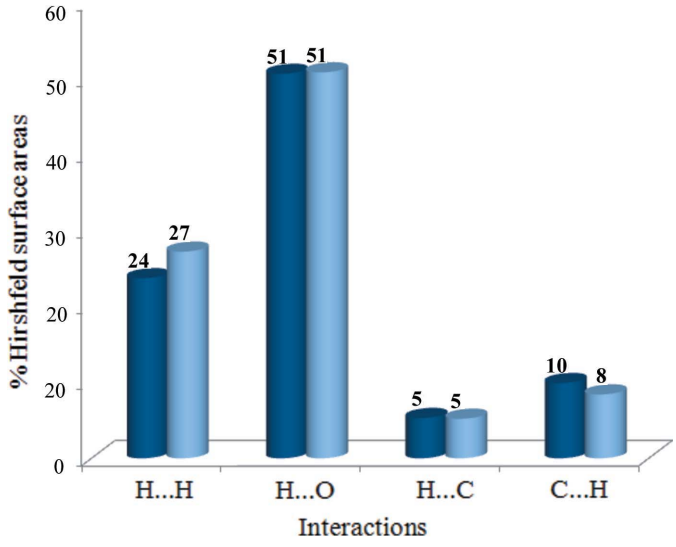

Figure 5
Relative contributions to the Hirshfeld surface areas for the various intermolecular contacts (H···H, H···O, H···C and C···H) in the dications of (I) (dark-blue columns) and (II) (light-blue columns). The N···O and C···O contacts (with negligible percentages of contact contributions) are not considered.

In FPs of cation–anion compounds, the contact regions between the HSs of the two species (cation and anion) in the asymmetric unit are visible, and it is possible to identify complementary regions in the FPs, where one component (cation) acts as an H-atom donor ($d_e > d_i$) and the other as an acceptor ($d_e < d_i$). The most striking of these complementary features is the broad green spike in the region $d_e > d_i$ on each of the full plots, resulting from the H···O contacts; similar spikes are not visible in the region $d_e < d_i$, due to the absence of O···H contacts. Moreover, the FPs in Fig. 4 clearly show the similarities, as well as the minor differences, between the distributions of interactions of the dications in (I) and (II).

Fig. 5 shows the relative contributions of the H···H, H···O, H···C and C···H contacts to the HS areas for the respective dications. By comparing the results in Fig. 5, it is seen that the H···O interactions outnumber the other contacts in the crystal structures (*versus* 0% area for the O···H interactions). Moreover, the percentages of the areas in Fig. 5 reveal that there are minor differences in the distributions of the H···H and C···H interactions for the dications of (I) and (II).

Support of this investigation by Ferdowsi University of Mashhad is gratefully acknowledged.

Supporting information for this paper is available from the IUCr electronic archives (Reference: LG3130).

References

Agilent (2010). *CrysAlis PRO*. Agilent Technologies, Yarnton, Oxfordshire, England.
Allen, F. H., Johnson, O., Shields, G. P., Smith, B. R. & Towler, M. (2004). *J. Appl. Cryst.* **37**, 335–338.

Bobbitt, J. M. (1998). *J. Org. Chem.* **63**, 9367–9374.
Brandenburg, K. & Putz, H. (2005). *DIAMOND*. Crystal Impact GbR, Bonn, Germany.
Burla, M. C., Camalli, M., Carrozzini, B., Cascarano, G. L., Giacovazzo, C., Polidori, G. & Spagna, R. (2003). *J. Appl. Cryst.* **36**, 1103.
Fabbiani, F. P. A., Arlin, J.-B., Buth, G., Dittrich, B., Florence, A. J., Herbst-Irmer, R. & Sowa, H. (2011). *Acta Cryst.* C**67**, o120–o124.
Gholizadeh, M., Maleki, B., Pourayoubi, M., Kia, M. & Notash, B. (2011). *Acta Cryst.* E**67**, o1614–o1615.
Gholizadeh, M., Pourayoubi, M., Kia, M., Rheingold, A. L. & Golen, J. A. (2012). *Acta Cryst.* E**68**, m305.
Ling, I., Alias, Y., Sobolev, A. N. & Raston, C. L. (2010). *CrystEngComm*, **12**, 4321–4327.
McKinnon, J. J., Spackman, M. A. & Mitchell, A. S. (2004). *Acta Cryst.* B**60**, 627–668.
Petříček, V., Dušek, M. & Palatinus, L. (2006). *JANA2006*. Institute of Physics, Prague, Czech Republic.
Rohl, A. L., Moret, M., Kaminsky, W., Claborn, K., McKinnon, J. J. & Kahr, B. (2008). *Cryst. Growth Des.* **8**, 4517–4525.
Spackman, M. A. & Byrom, P. G. (1997). *Chem. Phys. Lett.* **267**, 215–220.
Spackman, M. A. & Jayatilaka, D. (2009). *CrystEngComm*, **11**, 19–32.
Spackman, M. A. & McKinnon, J. J. (2002). *CrystEngComm*, **4**, 378–392.
Spek, A. L. (2009). *Acta Cryst.* D**65**, 148–155.
Tarahhomi, A., Pourayoubi, M., Golen, J. A., Zargaran, P., Elahi, B., Rheingold, A. L., Leyva Ramírez, M. A. & Mancilla Percino, T. (2013). *Acta Cryst.* B**69**, 260–270.
Wolff, S. K., Grimwood, D. J., McKinnon, J. J., Turner, M. J., Jayatilaka, D. & Spackman, M. A. (2012). *CrystalExplorer*. University of Western Australia, Australia.